A Multimode Supervisory Control Scheme for Coupling Remote Droop-Regulated Microgrids

Ehsan Pashajavid, Arindam Ghosh, *Fellow, IEEE* and Firuz Zare, *Senior Member, IEEE*

***Abstract*—This paper proposes a supervisory control scheme to facilitate coupling of remote droop-regulated microgrids (MGs) during power shortfalls. In this scheme, instead of power converters, an instantaneous static switch (ISS) is incorporated for the interconnection. Therefore a supervisory controller is essential to cope with the associated challenges, which are 1) the level of supporting power provided by the neighboring MG and 2) isolation procedure of the coupled MGs (CMG) when the power deficiency condition is removed. Droop coefficients of distributed generators (DGs) of the overloaded MG are dynamically updated by the controller according to the three operating modes defined to address the aforementioned challenges. The transit criteria, as well as the controlling signals, are accurately formulated based only on the local measurements to decrease the dependency on the communication systems. This enhances the reliability level of the coupled system. Effectiveness of the proposed strategy is validated through the results obtained from PSCAD/EMTDC simulations. Also, small-signal stability of the CMG operated by the proposed controller is examined using a developed model in MATLAB.**

***Index Terms*—Coupled Microgrids, Distributed Generation, Droop Regulator, Remote Area, Supervisory Control.**

I. Introduction

DISTRIBUTED generators (DG) are usually employed to supply electric demands of the rural and remote areas due to their isolation from main electricity networks [1]. Realization of such electrification systems can be fulfilled under the islanded microgrid (MG) framework [2]. Without any support from the main grid, the control of a remote MG can be much more complex than a grid-connected one. Droop control schemes are often utilized for regulating frequency and voltage of such isolated MGs along with proper load sharing amongst the DGs since the droop schemes show superior capabilities in operating based only on the local measurements [3-4]. As a result, costly and complicated communication infrastructures in remote areas can be avoided.

Power deficiency issue is one of the main challenges with remote MGs due to their limited power generation capacities [5-6]. Various strategies such as utilizing extra-sized diesel generators as well as employing energy storage systems were suggested in the literature to provide frequency support for an overloaded MG [7-8]. The stability of islanded MGs was enhanced in [9] through applying energy storage devices controlled by a hybrid droop method. With the aim of maintaining the supply-demand balance within an MG, a distributed cooperative control strategy was developed in [10] based on which the employed batteries were coordinated. The installation and operating costs of energy storage systems nevertheless are considerable. Also, fuel transport cost is one of the serious concerns with diesel generators that may expose remote MGs to high electricity prices or even, put them at the risk of supply interruption.

The concept of coupling neighboring MGs is recently presented that can be considered as an economically promising alternative since it imposes almost no extra capital investment [11-15]. In this concept, if an MG suffers from a power shortfall, while there is excess generation capacity in DGs of its neighboring MG, coupling these MGs to form a system of coupled MG (CMG) can relieve the overloading problem.

Interconnection of the MGs can be realized via back-to-back power converters that can control the active power flow [16-19]. However, the disadvantage of applying such converters is that they introduce additional losses in the system due to the conduction and switching losses of the semiconductor valves [20]. It is noticeable that the switching losses in back-to-back converters are consistent even during a zero power flow since they need to sustain the voltage across the DC capacitor connecting these two converters.

Alternatively, a CMG can be formed by closing a normally-open instantaneous static switch (ISS) mounted on the tie-line between the MGs. Considering a droop-based decentralized strategy, the required conditions and constraints to perform such interconnection procedures have been studied in [12]. Although employing the ISS under a communication-free framework can considerably decrease the total cost, it compromises controllability of the power flowing through the tie-line, and this, in turn, causes two major concerns with the performance of the system as explained below

1) By forming a CMG, a supporting power is supplied by the neighboring MG that relieves the shortfall. Since the DGs of both the MGs share the total load of the system as per their power capacities, the power output of the DGs of the overloaded MG may be less than their maximum allowable limits. In other words, the supporting power is probably larger than the actual requirement of the MG experiencing the power shortfall. This undesirable consequence can impose extra costs on the MG owner. Note that, as a desirable power exchange criterion, the overloaded MG should generate its maximum allowable power while the neighboring MG should only supply the rest of the load demand.
2) Once the power shortfall is removed, the MGs should isolate to carry on their normal operation independently. Due to the dissimilar configuration of the MGs, however, a non-zero

E. Pashajavid and A. Ghosh are with the Department of Electrical and Computer Engineering, Curtin University, Perth, Australia.

Firuz Zare is with Power Engineering Group, University of Queensland, Brisbane, Australia.

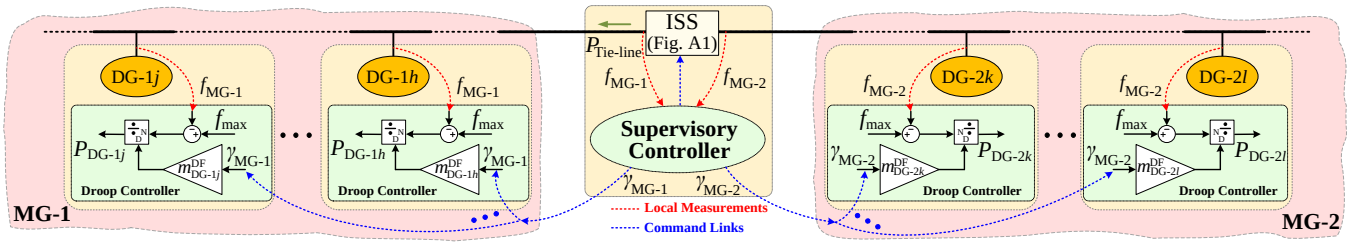

Fig. 1 The network of two remote neighboring microgrids.

power may still flow through the tie-line. In this case, improper isolation of the MGs can impose considerable voltage spikes on the ISS that may damage the device or decrease its lifetime.

This paper proposes a supervisory control scheme to facilitate ISS-based coupling of the neighboring MGs, as well as, a proper isolation strategy for the coupled MGs. In order to address the above-mentioned challenges, operation of the developed strategy is conducted under three different modes – namely, Mode 1: that is initiated by forming the CMG to sustain the power output of the overloaded MG close to its maximum, Mode 2: that aims to fulfill a successful isolation when the interconnection is not required anymore and Mode 3: that starts by opening the ISS to reset default values of the DG primary controllers. The ISS controller is responsible for implementing the developed scheme by appropriately modifying the droop coefficients of the DGs located within the overloaded MG.

The supervisory scheme proposed in this paper aims at driving the ISS-based CMG system from the current to a desired operating point while maintaining the reliability and simplicity of the network by avoiding complex communication systems. The major features of the proposed scheme can be summarized as follows:

1) Since the scheme operates based on only the local measurement (e.g. MG frequencies and tie-line power), it does not need to collect any information of the system via a communication infrastructure.
2) The scheme affects DGs of the overloaded MG only, avoiding to interfere in local regulating actions of the supporting MG.
3) The whole supervisory action is fulfilled merely by applying a single controlling parameter. Consequently, the implementation of the scheme is straightforward.
4) A very low bandwidth unidirectional communication system is needed to send the same supervisory parameter to the DGs of the overloaded MG.
5) The scheme can efficiently regulate level of the power transfer between the MGs of the ISS-based CMG system in accordance with the defined criteria.
6) The scheme is capable of implementing a disturbance-free isolation even under dissimilar loading levels of the MGs.

The rest of this paper is organized as follows. Section II describes the general concept of droop regulation. The challenges with an ISS-based CMG are discussed in Section III. The proposed supervisory scheme to address the challenges is presented in Section IV. In Section V, the developed small-signal model for eigenvalue analysis is explained. Section VI appraises performance of the scheme based on outcomes of the conducted simulations. Section VII concludes this paper.

II. Droop Regulation

Let us consider the two neighboring remote MGs of Fig. 1 consisting of N_1 and N_2 droop-controlled DGs. The frequency and voltage at the output of each DG are regulated by droop control as [4]

$$f = f_{\max} - m_{\text{DG}} P_{\text{DG}} \quad , \quad V = V_{\max} - n_{\text{DG}} Q_{\text{DG}} \tag{1}$$

where $f_{\max}$ and $V_{\max}$ are respectively the rated frequency and voltage magnitude in the MG, P_{DG} and Q_{DG} are respectively the active and reactive powers injected by the DG and m_{DG} and n_{DG} are respectively the P–f and Q–V droop coefficients derived from

$$m_{\text{DG}} = (f_{\max} - f_{\min}) / P^{\text{cap}}_{\text{DG}} \ , \ n_{\text{DG}} = (V_{\max} - V_{\min}) / Q^{\text{cap}}_{\text{DG}} \tag{2}$$

where superscript cap indicates power capacity of each DG and $f_{\min}$ and $V_{\min}$ are respectively the minimum of frequency and voltage magnitude in the MG. As illustrated in Fig. 1, the DGs of each MG can have different droop coefficients since their power capacities can be dissimilar. The load sharing between any two DGs e.g. i^{th} and j^{th}, is fulfilled according to their droop coefficients as follows

$$\frac{P_{\text{DG-}i}}{P_{\text{DG-}j}} = \frac{m_{\text{DG-}j}}{m_{\text{DG-}i}} \rightarrow \frac{P_{\text{DG-}i}}{P_{\text{DG-}j}} = \frac{P^{\text{cap}}_{\text{DG-}i}}{P^{\text{cap}}_{\text{DG-}j}} \tag{3}$$

The MGs can be interconnected by closing the ISS mounted on the tie-line, as can be seen from Fig. 1. The ISS controller manages the interconnection using only the local measurements.

Droop equations (1) should be adopted when the line impedances are inductive. Otherwise, proper decoupling between active and reactive powers cannot be achieved [16]. Therefore, the interfacing inductances of the DGs, L_{DG}, in the network of Fig. 1 should be chosen large enough in comparison to those of the lines, in order to avoid this negative impact on power sharing. Let us consider the suitable criterion for size selection of L_{DG} as $L_{\text{DG}}\omega > (5\sim10)\times|Z_{\text{line}}|$ where ω is the system frequency and Z_{line} represents the line impedances. Note that the maximum output power of each DG sets the upper limit for the size of its L_{DG}.

Due to the reason mentioned above, the active power can be regulated well by (1). Accurate sharing of reactive power nevertheless can face challenges. Since the main focus of this paper is addressing the active power shortfalls in isolated MGs, it is assumed that the reactive term of the loads can be mainly supplied by local reactive power compensators. Thus, adopting (1) for DGs of the network shown in Fig. 1 is sensible as it can maintain simplicity of the system while performing the required power regulation. Under extreme situations, however, more complex techniques of droop control should be employed

[21].

In [22], small signal stability performance of a CMG is studied for various selections of different interconnection buses when the coupling inductances of the DGs are in the same range of the lines. The results show that the stability margin of the CMG can be considerably sensitive to the impedances of the lines and tie-line. This, in turn, can lead to strong variations in the performance of the CMG both in terms of stability and transient response. In contrast, eigenvalue analysis of a CMG is performed in [12] for different combinations of the tie-line impedance when the DG interfacing inductances are selected adequately high in comparison to those of the lines. The outcomes reveal that variations in the tie-line impedance of the considered CMG does not cause instability under any of the simulated scenarios.

Therefore, another advantage of proper design of the DGs to meet the aforementioned size constraint on the output inductances is to enhance droop gain stability margin of the whole system and to extend the range of its insensitivity to various impedance combinations of the CMG lines. Consequently, the performance of the CMG can be satisfactory both in terms of stability and transient response. Further discussions are provided in Section IV.B.

III. Problem Statement

Interconnection of the neighboring MGs can be a promising alternative to traditional frequency support techniques, mainly in remote areas rich in renewable resources. Let us consider the system of two isolated MGs shown in Fig. 1 in which DGs of each MG are regulated by droop control with the same maximum frequency deviations. By forming the CMG system the total load will be shared by DGs of the both MGs. The criteria for the interconnection as well as the isolation procedures are briefly presented in this section. Then, the concerns with the communication-free operation of the CMG are fully discussed.

A. Coupling and isolation conditions

Let us assume that MG-1 experiences a power shortfall if its frequency, $f_{\text{MG-1}}$, drops below a threshold defined as [12-13]

$$f_{\text{MG-1}} < f_{\min} + \alpha(f_{\max} - f_{\min}) \tag{4}$$

where $0<\alpha<1$. From (1) and (2), (4) implies that if $f_{\text{MG-1}}$ meets the above condition, the unused power capacity (UPC) of MG-1 is less than α times the total power capacity of all DGs of MG-1, $P^{\text{cap}}_{\text{MG-1}} = \sum_{i=1}^{N_1} P^{\text{cap}}_{\text{DG-}i}$, i.e.

$$P^{\text{cap}}_{\text{MG-1}} - P_{\text{MG-1}} < \alpha P^{\text{cap}}_{\text{MG-1}} \rightarrow P_{\text{MG-1}} > (1-\alpha)P^{\text{cap}}_{\text{MG-1}} \tag{5}$$

where $P_{\text{MG-1}}$ is the total power output of all DGs of MG-1. For example, assuming α=0.1, MG-1 is overloaded if its UPC is less than 10% of its power capacity. In this case, the controller commands the ISS to close provided that the interconnection will not cause power deficiency in MG-2, i.e.,

$$P_{\text{CMG}} < (1-\alpha)P^{\text{cap}}_{\text{CMG}} \tag{6}$$

where $P_{\text{CMG}} = P_{\text{MG-1}} + P_{\text{MG-2}}$ and $P^{\text{cap}}_{\text{CMG}} = P^{\text{cap}}_{\text{MG-1}} + P^{\text{cap}}_{\text{MG-2}}$. It can be proved that this constraint is satisfied if the frequency of MG-2, $f_{\text{MG-2}}$, meets the following criterion

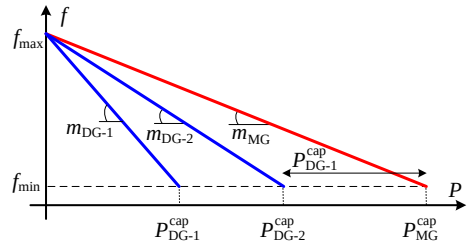

Fig. 2. Equivalent droop curve of an MG along with droop curves of its DGs.

$$f_{\text{MG-2}} > f_{\max} - m_{\text{MG-2}} \times \left[(1-\alpha) \times (P^{\text{cap}}_{\text{MG-1}} + P^{\text{cap}}_{\text{MG-2}}) - \frac{f_{\max} - f_{\text{MG-1}}}{m_{\text{MG-1}}} \right] \tag{7}$$

where m_{MG} indicates the equivalent droop coefficient of all DGs of an MG explained as

$$m_{\text{MG}} = 1 \Big/ \sum_{i=1}^{N} \frac{1}{m_{\text{DG-}i}} \tag{8}$$

Fig. 2 illustrates the equivalent droop curve of an MG containing only two DGs. This figure shows how the two DGs can be aggregated by a single unit representing the droop behavior of the MG. Similar to (2), m_{MG} can also be defined as

$$m_{\text{MG}} = (f_{\max} - f_{\min}) / P^{\text{cap}}_{\text{MG}} \tag{9}$$

The ISS controller initiates the interconnection if both (4) and (7) are satisfied. Then, the ISS closes when the voltages at its two sides are synchronized.

After forming the CMG system, a supporting power of $P_{\text{Tie-line}}$ flows through the tie-line towards MG-1. Using (1), (2) and (4), it can be shown that MG-1 requires receiving the support from MG-2 as long as $P_{\text{Tie-line}}$ can be expressed as

$$P_{\text{Tie-line}} > (1-\alpha) \times P^{\text{cap}}_{\text{MG-1}} - (f_{\max} - f_{\text{CMG}}) / m_{\text{MG-1}} \tag{10}$$

where f_{CMG} indicates the frequency of the CMG. However, the interconnection is no longer required in case $P_{\text{Tie-line}}$ drops below the above limit. In other words, the violation of (10) means the state of power deficiency in MG-1 is already removed, and hence, the MGs should be isolated.

It is worthy to emphasis that (4), (7) and (10) are based on only the local measurements at the ISS.

B. Challenges with the communication-free CMG

Two undesirable features of forming a CMG system using an ISS under a fully decentralized structure are as follows

1) The level of supporting power

From MG-1 owner's point of view, the power exchange is desirable if $P_{\text{Tie-line}}$ can be expressed as

$$P^{\text{DSR}}_{\text{Tie-line}} = P^{\text{Load}}_{\text{MG-1}} - P^{\text{DSR}}_{\text{MG-1}}, \quad P^{\text{DSR}}_{\text{MG-1}} = (1-\alpha)P^{\text{cap}}_{\text{MG-1}} \tag{11}$$

where $P^{\text{Load}}_{\text{MG-1}}$ is the total load of MG-1 while $P^{\text{DSR}}_{\text{MG-1}}$ indicates the desired power output of MG-1 during the interconnection. Equation (11) implies that the supporting power should be limited to the portion of $P^{\text{Load}}_{\text{MG-1}}$ that cannot be met by the DGs of MG-1. By forming the CMG, however, the total load of the system, $P^{\text{Load}}_{\text{CMG}} = P^{\text{Load}}_{\text{MG-1}} + P^{\text{Load}}_{\text{MG-2}}$, is shared by DGs of the both MGs in accordance with the ratios stated in (3). Thus, the total power output of MG-2 can be described as

$$P_{\text{MG-2}} = (P^{\text{cap}}_{\text{MG-2}} / P^{\text{cap}}_{\text{MG-1}}) P_{\text{MG-1}} \tag{12}$$

This is because the CMG is actually a larger MG containing N_1+N_2 droop-regulated DGs. As already mentioned, the

satisfaction of (7) guarantees that the UPC of the CMG can be stated as (6). Substitution of (12) in (6) yields

$$P_{\text{MG-1}} + \frac{P^{\text{cap}}_{\text{MG-2}}}{P^{\text{cap}}_{\text{MG-1}}} P_{\text{MG-1}} < (1-\alpha) P^{\text{cap}}_{\text{CMG}} \rightarrow P_{\text{MG-1}} < (1-\alpha) P^{\text{cap}}_{\text{MG-1}} \quad (13)$$

which means the power output of MG-1 is now less than $P^{\text{DSR}}_{\text{MG-1}}$, causing the resultant supporting power to be larger than $P^{\text{DSR}}_{\text{Tie-line}}$.

2) Isolation procedure

According to the Thevenin equivalent of the CMG system, the voltage across the ISS can be stated as

$$v_{\text{ISS}}(t) = L_{\text{Eq}} \frac{di_{\text{Tie-line}}(t)}{dt} + R_{\text{Eq}} i_{\text{Tie-line}}(t) + v_{\text{Eq-MGs}}(t) \quad (14)$$

where L_{Eq} and R_{Eq} respectively are the equivalent inductance and the resistance of the system seen from the ISS. Also, $v_{\text{Eq-MGs}}$ and $i_{\text{Tie-line}}$ denote the resultant voltage of the MGs and the tie-line current respectively.

Although the violation of (10) indicates the necessity of an isolation action, a considerable power may still pass through the ISS due to the droop-based load sharing of the DGs. Because of the derivative term of (14), opening the ISS under this condition may cause destructive transients, damaging the device or decreasing its lifetime. Therefore, a proper mechanism should be developed to facilitate a successful isolation procedure such that neither the ISS nor the other components of the system are damaged.

IV. The Proposed Supervisory Scheme

As explained in Section III.B, the ISS-based CMG forming procedure by adopting pre-specified coefficients of the droop regulators may yield undesirable consequences. In this section, the mentioned challenges are addressed by developing a supervisory control scheme that achieves the defined goals by updating the droop coefficients of the overloaded MG during the interconnection. The scheme is embedded in the ISS controller to complement its performance described in Section III.A. The supervisory action is fulfilled based on three operating modes appropriately defined for the scheme as shown in Fig. 3. Using only the local measurements, the controller switches to the proper mode and consequently readjusts the droop coefficients of the DGs. Fig. 4 shows the flowchart based on which the controller applies the scheme. The defined modes along with the associated transition criteria are discussed in detail in the following subsections. From this point on, $m^{\text{DF}}_{\text{DG}}$ and $m^{\text{DF}}_{\text{MG}}$ indicate the default droop coefficient of a DG as (2) and an MG as (9) respectively while m_{DG} and m_{MG} are the ones updated by the controller.

A. Mode 1: Coupling

The first operating mode is designed to address the concern with the level of supporting power provided by the neighboring MG, as explained in Section III.B.1. Once the CMG is formed, the DGs of MG-1 should be forced to deliver $P^{\text{DSR}}_{\text{MG-1}}$ while the rest of its demand can be supported by the neighboring MG ($P^{\text{DSR}}_{\text{Tie-line}}$). In order to achieve this goal, from (3) and (11), the power outputs of the MGs are to satisfy a load sharing ratio as

$$\frac{P^{\text{DSR}}_{\text{MG-1}}}{P_{\text{MG-2}}} = \frac{m^{\text{DF}}_{\text{MG-2}}}{m_{\text{MG-1}}} \quad (15)$$

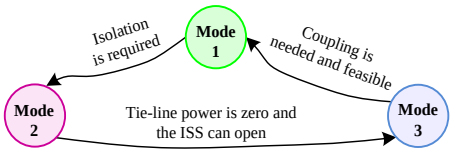

Fig. 3 Operating modes of the developed scheme.

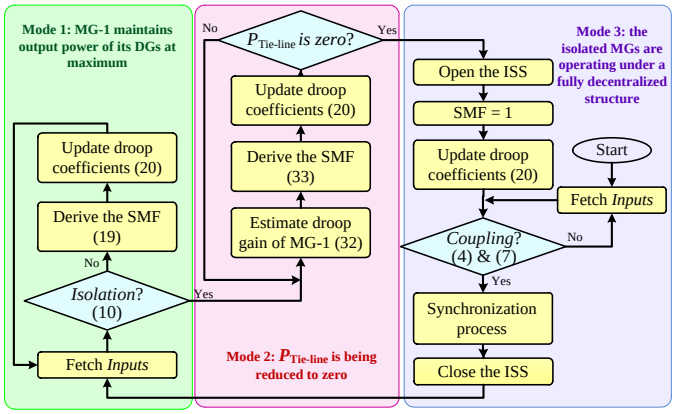

Fig. 4 Operation flowchart of the proposed scheme.

Therefore, the equivalent droop coefficient of MG-1 needs to be readjusted as

$$m_{\text{MG-1}} = \frac{m^{\text{DF}}_{\text{MG-2}} \times P_{\text{MG-2}}}{(1-\alpha) P^{\text{cap}}_{\text{MG-1}}} \quad (16)$$

By dynamically applying (16), power outputs of the DGs of MG-1 can be always maintained at their maximum. Now, let us define the slope modification factor (SMF) as

$$\gamma = m_{\text{MG}} / m^{\text{DF}}_{\text{MG}} \quad (17)$$

which is the supervisory coefficient of the system. The main idea is to extract the proper SMFs based on which the controller can update droop coefficients of the DGs desirably. Note that the dependency levels on the communication system should be decreased in order to enhance the CMG reliability. This means the operation of the controller should be mostly based on the local measurements, i.e. f_{CMG} and $P_{\text{Tie-line}}$. To achieve this goal, using (1), (16) is restated as

$$m_{\text{MG-1}} = \frac{f_{\max} - f_{\text{CMG}}}{(1-\alpha) P^{\text{cap}}_{\text{MG-1}}} \quad (18)$$

Note that m_{MG} is the modified droop coefficient of the MG and $m^{\text{DF}}_{\text{MG}}$ is the default value of the droop coefficient expressed in (9). Hence, substituting (9) and (18) in (17) yields the SMF to be sent to MG-1 as

$$\gamma_{\text{MG-1}} = \frac{f_{\max} - f_{\text{CMG}}}{(1-\alpha) P^{\text{cap}}_{\text{MG-1}}} \Big/ \frac{(f_{\max} - f_{\min})}{P^{\text{cap}}_{\text{MG-1}}} = \frac{1}{1-\alpha} \times \frac{f_{\max} - f_{\text{CMG}}}{f_{\max} - f_{\min}} \quad (19)$$

Equation (19) is capable of yielding the SMF only by measuring the CMG frequency at the ISS. Whenever the SMF is updated by the controller, the DGs of MG-1 should modify their droop coefficients accordingly as follows

$$m_{\text{DG-1}i} = \gamma_{\text{MG-1}} \times m^{\text{DF}}_{\text{DG-1}i} \quad (20)$$

where $i \in \{1, \ldots, N_1\}$. Eventually, the droop regulator of each DG should be altered as

$$f_{\text{CMG}} = f_{\max} - \gamma_{\text{MG-1}} \times m^{\text{DF}}_{\text{DG-1}i} P_{\text{DG-1}i} \quad (21)$$

as shown in Fig. 1. By adaptively adjusting the SMF, and thereby the droop coefficients, the controller ensures that the

DGs of MG-2 provide MG-1 with $P^{\text{DSR}}_{\text{Tie-line}}$.

In order to provide further insight into the mechanism of the approach, let us consider droop curves of a sample CMG shown in Fig. 5 where f_α is the threshold frequency defined in (4) and f_1 is the CMG frequency when the supervisory scheme is not included. Without loss of generality, the capacity of MG-2 is assumed to be larger than that of MG-1. Since the power output of MG-1 at f_1 is definitely less than $P^{\text{DSR}}_{\text{MG-1}}$ (see (13)), extra supporting power is undesirably provided by MG-2. By activating the scheme, the controller calculates regularly the appropriate SMF by using (19), which only needs frequency measurement at the ISS. Then, the SMF is sent to the DGs using a very low bandwidth communication system to update the droop coefficients as per (20). Consequently, $P_{\text{MG-2}}$ can be successfully decreased through increasing $P_{\text{MG-1}}$ to $P^{\text{DSR}}_{\text{MG-1}}$, as can be seen from Fig. 5, reducing the supporting power to $P^{\text{DSR}}_{\text{Tie-line}}$. From the CMG point of view, the power capacity of MG-1 is virtually increased to

$$P^{\text{Vcap}}_{\text{MG-1}} = \frac{f_{\max} - f_{\min}}{f_{\max} - f_{\text{CMG}}} P^{\text{DSR}}_{\text{MG-1}} \tag{22}$$

This leads to the frequency increase to f_2 as $m^{\text{DF}}_{\text{MG}}$ is decreased to $m_{\text{MG-1}}$ (see (9)). As long as Mode 1 of the scheme is active, $P^{\text{DSR}}_{\text{MG-1}}$ is the power output locus of MG-1, as shown in Fig. 5.

B. Mode 2: Canceling the tie-line power

The ISS controller is responsible for implementing the isolation action under a quasi-decentralized scheme. This means the developed scheme should be capable of handling the issue raised in Section III.B.2 by extracting proper SMF values. The target is to decrease $P_{\text{Tie-line}}$ to about zero before opening the ISS such that the destructive transients caused by the derivative term of (14) can be avoided. This section begins with examining the condition under which no supporting power flows through the ISS. Then, the supervisory approach to achieve this condition is presented.

1) Load-to-capacity ratio

Let us assume the ISS controller is operating under a fully decentralized structure which means no supervisory action is present. By forming a CMG, the total load of the system, $P^{\text{Load}}_{\text{CMG}}$, is shared by DGs of the MGs in accordance with the ratios stated in (3). Assuming

$$P^{\text{cap}}_{\text{MG-1}} / P^{\text{cap}}_{\text{MG-2}} = \eta \tag{23}$$

the total power output of the MGs can be expressed as

$$P_{\text{MG-1}} = \frac{\eta}{\eta+1} P^{\text{Load}}_{\text{CMG}},\ P_{\text{MG-2}} = \frac{1}{\eta+1} P^{\text{Load}}_{\text{CMG}} \tag{24}$$

Using (24), $P_{\text{Tie-line}}$ (as shown in Fig. 1) can be derived as

$$P_{\text{Tie-line}} = \frac{1}{\eta+1} P^{\text{Load}}_{\text{CMG}} - P^{\text{Load}}_{\text{MG-2}} \tag{25}$$

Now, let us define the load-to-capacity (L2C) ratio of an MG as

$$\text{L2C}_{\text{MG}} = P^{\text{Load}}_{\text{MG}} / P^{\text{cap}}_{\text{MG}} \tag{26}$$

Assuming the violation of (10), the following two scenarios are relevant:

- The L2C ratios of the MGs are identical i.e. $P^{\text{Load}}_{\text{MG-1}} / P^{\text{Load}}_{\text{MG-2}} = P^{\text{cap}}_{\text{MG-1}} / P^{\text{cap}}_{\text{MG-2}}$. From (23), the total load of the system can be described as

$$P^{\text{Load}}_{\text{CMG}} = (\eta+1) \times P^{\text{Load}}_{\text{MG-2}} \tag{27}$$

Replacing (27) in (25) concludes that if the MGs have the same L2C ratios, $P_{\text{Tie-line}}$ becomes zero. Thus, the isolation can be fulfilled without any transient.

- The L2C ratios of the MGs are different. This condition yields a non-zero $P_{\text{Tie-line}}$ of (25), causing the undesirable disturbances across the ISS at the isolation, as explained in Section III.B.2.

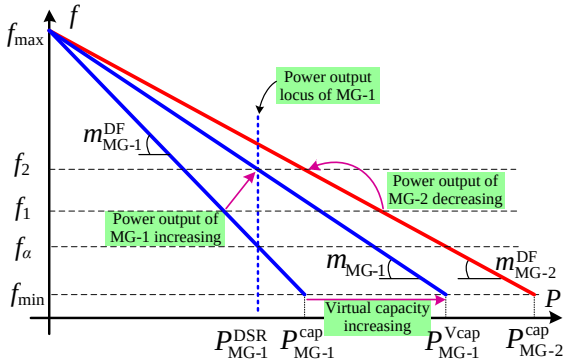

Fig. 5. Performance of the developed supervisory scheme under Mode 1.

2) The supervisory action under Mode 2

In order to achieve a successful disturbance-free isolation, therefore, an L2C equalization procedure should be performed. Due to the fact that the controller has no direct access to the loads, the equalization should be implemented by virtually modifying the power capacity of MG-1. From (26), the L2C equalization can be attained if the virtual capacity of MG-1 can be ideally expressed as

$$P^{\text{Vcap}}_{\text{MG-1}} = \frac{P^{\text{Load}}_{\text{MG-1}}}{P^{\text{Load}}_{\text{MG-2}}} P^{\text{cap}}_{\text{MG-2}} \tag{28}$$

According to the direction of $P_{\text{Tie-line}}$ shown in Fig. 1, the total load demand of the MGs can be described by

$$P^{\text{Load}}_{\text{MG-1}} = P_{\text{MG-1}} + P_{\text{Tie-line}},\ P^{\text{Load}}_{\text{MG-2}} = P_{\text{MG-2}} - P_{\text{Tie-line}} \tag{29}$$

Substituting (29) in (28) yields

$$P^{\text{Vcap}}_{\text{MG-1}} = \frac{P_{\text{MG-1}} + P_{\text{Tie-line}}}{P_{\text{MG-2}} - P_{\text{Tie-line}}} P^{\text{cap}}_{\text{MG-2}} \tag{30}$$

Thus, by redefining the droop coefficient of MG-1 utilizing the virtual capacity of (30), the DGs of MG-1 can successfully modify their power outputs to drop the tie-line power to zero. However, (30) depends on the simultaneous measurement of power outputs of the DGs of both MGs using appropriate power sensors that necessitates a high bandwidth bidirectional communication system, compromising reliability as well as increasing complexity and the total cost of the system. This issue can be efficiently addressed by restating (30) using the droop equations of (1) and (9) as

$$P^{\text{Vcap}(k)}_{\text{MG-1}} = \frac{f_{\max} - f_{\min}}{m^{(k-1)}_{\text{MG-1}}} \times \frac{f_{\max} - f_{\text{CMG}} + m^{(k-1)}_{\text{MG-1}} \times P_{\text{Tie-line}}}{f_{\max} - f_{\text{CMG}} - m^{\text{DF}}_{\text{MG-2}} \times P_{\text{Tie-line}}} \tag{31}$$

where $P^{\text{Vcap}(k)}_{\text{MG-1}}$ represents the virtual capacity of MG-1 at step k while $m^{(k-1)}_{\text{MG-1}}$ is the droop coefficient of MG-1 at step $k-1$. Therefore, $m_{\text{MG-1}}$ at step k can be derived as

$$m_{\text{MG-1}}^{(k)} = m_{\text{MG-1}}^{(k-1)} \times \frac{f_{\max} - f_{\text{CMG}} - m_{\text{MG-2}}^{\text{DF}} \times P_{\text{Tie-line}}}{f_{\max} - f_{\text{CMG}} + m_{\text{MG-1}}^{(k-1)} \times P_{\text{Tie-line}}} \quad (32)$$

Replacing (32) in (17) yields the SMF command as

$$\gamma_{\text{MG-1}}^{(k)} = \frac{m_{\text{MG-1}}^{(k-1)}}{m_{\text{MG-1}}^{\text{DF}}} \times \frac{f_{\max} - f_{\text{CMG}} - m_{\text{MG-2}}^{\text{DF}} \times P_{\text{Tie-line}}}{f_{\max} - f_{\text{CMG}} + m_{\text{MG-1}}^{(k-1)} \times P_{\text{Tie-line}}} \quad (33)$$

Note that $m_{\text{MG-1}}^{(0)}$ is the last value of $m_{\text{MG-1}}$ derived by (18) during Mode 1. Now employing (33), the controller can iteratively update the SMF by only measuring the CMG frequency and the tie-line power at the ISS. Therefore, the DGs of MG-1 are ordered to readjust their droop coefficients accordingly as (20), intending to reduce the passing power through the ISS. Eventually, the controller sends a command to the ISS to open once the tie-line power drops to zero. Note that the step size can be determined in accordance with the dynamic response of the MG as well as the bandwidth of the communication system.

Let the change between droop coefficients of MG-1 at two consecutive steps be expressed as

$$\Delta^{(k)} = m_{\text{MG-1}}^{(k)} - m_{\text{MG-1}}^{(k-1)} \quad (34)$$

If the error $\Delta^{(k)}$ tends to zero, then $P_{\text{Tie-line}}$ also approaches the desired value of $P_{\text{Tie-line}}$=0. Let us assume (10) is violated following a load change in MG-1; however, Mode 2 is not activated yet. Considering the direction of $P_{\text{Tie-line}}$ in Fig. 1, the following scenarios are relevant:

- $P_{\text{Tie-line}}$ is positive which means the total generation of MG-1, $P_{\text{MG-1}}$, is still lower than its total load. In this case, employing (32) at each step causes a relative reduction in the droop slope of MG-1, which, in turn, results in increasing $P_{\text{MG-1}}$ (see (3)), decreasing $P_{\text{Tie-line}}$. Carrying on this procedure can ultimately drop Δ to zero, canceling the tie-line power.
- If the total generation of MG-1 is now larger than its load, the violation of (10) is followed by a negative $P_{\text{Tie-line}}$. Thus, applying the supervisory scheme of Mode 2 increases the droop slope of MG-1 to decrease $P_{\text{MG-1}}$, reducing the tie-line power step by step. Note that Δ decreases by dropping $P_{\text{Tie-line}}$. This ensures that the scheme can successfully achieve its goal.

C. Mode 3: Isolation

As soon as $P_{\text{Tie-line}}$ reduces to zero, the ISS can open to isolate the MGs with no destructive transients. By opening the ISS, the droop coefficients of MG-1 should be reset to their default values. This task can be done by sending an SMF of

$$\gamma_{\text{MG-1}} = 1 \quad (35)$$

to the DGs, retrieving their normal droop regulation. Now the supervisory action is not required anymore and the two isolated MGs can carry on their operation independently under a communication-free structure. In other words, as long as the ISS is open and no power shortfall is detected, the supervisory controller stays idle and does not interfere in the normal operation of the MGs.

According to Section III.A, two sets of conditions are defined, namely the coupling conditions formulated as (4) and (7), and the isolation condition formulated as (10). As illustrated in flowchart of Fig. 4, the coupling conditions are included in Mode 3 of the proposed scheme. After opening the ISS and resetting the droop coefficient of the DGs to their default values, the controller should monitor the frequencies regularly to detect the next overloading. This action is implemented via the loop included in flowchart of Mode 3 shown in Fig. 4. In case of a power deficiency in one of the MGs, i.e., when (4) is met, the controller initiates the synchronization and interconnection procedures subject to availability of sufficient surplus generation in the neighboring MG, i.e., if (7) is satisfied as well. Afterwards, the controller executes the supervisory actions through activating Mode 1. On the other hand, the algorithm carries on the operation within the mentioned loop if any of the coupling conditions is not satisfied. It is to be noted that the transient-free interconnection procedure of the MGs has already been presented in [12].

D. Overall description

This paper aims at developing a supervisory control scheme to modify the droop coefficients of the DGs within an overloaded MG for regulating the amount of supporting power provided by its neighboring MG. This target should be attained with lower dependency on the communication systems in order to enhance reliability of the formed CMG. Therefore, a supervisory scheme is proposed based on a single parameter called the SMF, γ, capable of being implemented via a unidirectional low bandwidth communication system to modify the droop coefficients of the DGs properly for the overloaded MG in accordance with the defined operating modes. In brief, the following steps can express algorithm used by the controller:

i. Set the operating mode based on the fetched inputs and the ISS status.
ii. Calculate the appropriate SMF using (19), (33) and (35) for Modes 1, 2 and 3 respectively.
iii. Send the SMF to all DGs within the overloaded MG.

Then, each DG should apply the SMF on its own droop regulator as (21) to achieve the desired target. It is to be mentioned again that all DGs within the overloaded MG receive the same SMF. This identical SMF is called $\gamma_{\text{MG-1}}$ when the overloaded MG is MG-1 and $\gamma_{\text{MG-2}}$ if MG-2 is overloaded.

Note that, without loss of generality, the scheme is described assuming MG-1 is overloaded and MG-2 is the supporting MG. However, if MG-2 is overloaded and MG-1 is the supporting one, the extracted formulations can be straightforwardly applied by exchanging the subscripts.

V. Small Signal Stability Analysis

The small-signal analysis is carried out by augmenting the model of [12,23] to consider the effect of the SMF. However, derivation procedure of [12,23] is not mentioned here due to space limitations. The angular frequency of each DG (ω) with respect to a common angular frequency (ω_{com}) (i.e. the angular frequency of one of the DGs) can be expressed as

$$\delta = \int (\omega - \omega_{\text{com}})\, dt \quad (36)$$

From (21), ω is described as

$$\omega = \omega_{\max} - 2\pi \times \gamma \times m_{\text{DG}}^{\text{DF}} P_{\text{DG}} \quad (37)$$

Replacing (37) in (36) and then, linearizing the result yields

$$\Delta\dot{\delta}/2\pi = m_{\text{com}}^{\text{DF}} \gamma^{\text{o}} \Delta P_{\text{com}} + \left(m_{\text{com}}^{\text{DF}} P_{\text{com}}^{\text{o}} - m_{\text{DG}}^{\text{DF}} P_{\text{DG}}^{\text{o}}\right)\Delta\gamma - m_{\text{DG}}^{\text{DF}} \gamma^{\text{o}} \Delta P_{\text{DG}} \quad (38)$$

where P_{com} and m_{com} represent power output and droop slope of the reference DG respectively, and superscript o indicates the value at the operating point. Taking into account (38), it can be

shown that for a CMG formed by the two interconnected MGs, the linearized state-space equation can be described as (39) in which $x_{MG\text{-}i}$ includes the state variables of MG-*i* and $v_{MG\text{-}i}$ shows the buses voltages of MG-*i*.

$$\begin{bmatrix} \Delta\dot{x}_{MG-1} \\ \Delta\dot{x}_{MG-2} \\ \Delta\dot{x}_{Tie-line} \end{bmatrix} = \begin{bmatrix} A_{MG-1} & O_{Ns1\times Ns2} & O_{Ns1\times 2} \\ O_{Ns2\times Ns1} & A_{MG-2} & O_{Ns2\times 2} \\ O_{2\times Ns1} & O_{2\times Ns2} & A_{Tie-line} \end{bmatrix} \begin{bmatrix} \Delta x_{MG-1} \\ \Delta x_{MG-2} \\ \Delta x_{Tie-line} \end{bmatrix} + \begin{bmatrix} B_{MG-1} & O_{Ns1\times(2\times Nb2)} \\ O_{Ns2\times(2\times Nb1)} & B_{MG-2} \\ \hline B_{Tie-line} \end{bmatrix} \begin{bmatrix} \Delta v_{MG-1} \\ \Delta v_{MG-2} \end{bmatrix} \quad (39)$$

All parameters are expressed in the common d-q reference frame. It is to be noted that for MG-*i* with N_{DG} DGs, N_d loads, N_L lines and N_b buses, the number of states, Ns-*i*, is $10N_{DG}+2N_L+2N_d$ while the tie-line has two states, i.e., $x_{MG\text{-}1}$, $x_{MG\text{-}2}$ and $x_{Tie\text{-}line}$ are vectors with Ns1, Ns2 and 2 elements respectively, while $v_{MG\text{-}1}$ and $v_{MG\text{-}2}$ have, respectively, $2N_{b1}$ and $2N_{b2}$ elements. In (39), $O_{a\times b}$ is a zeros matrix of *a* rows and *b* columns, and $A_{MG\text{-}1}$, $A_{MG\text{-}2}$ and $A_{Tie\text{-}line}$ are matrixes of order Ns1×Ns1, Ns2×Ns2 and 2×2 respectively. Also, $B_{MG\text{-}1}$, $B_{MG\text{-}2}$ and $B_{Tie\text{-}line}$ are matrixes of order Ns1×2Nb1, Ns2×2Nb2 and 2×2(Nb1+Nb2), respectively.

In order to obtain the homogeneous form of the state space representation of the CMG, the node voltages have to be eliminated from (39). Since $[\Delta v_{MG\text{-}1} \;\; \Delta v_{MG\text{-}2}]^T = M.\Delta x_{CMG}$ [23], (39) can be restated in the form of

$$\Delta\dot{x}_{CMG} = A_{CMG}\,\Delta x_{CMG} \quad (40)$$

where $x_{CMG} = [x_{MG\text{-}1} \;\; x_{MG\text{-}2} \;\; x_{Tie\text{-}line}]^T$ and A_{CMG} is the state matrix of the CMG. Now, the eigenvalues of the CMG can be calculated from (40).

VI. Performance Evaluation

In order to appraise the performance of the developed scheme, relevant simulation case studies are carried out in PSCAD/EMTDC. Consider the network of Fig. 1 with the structure described in Section II. The detailed technical parameters of the network and the schemes can be found in Appendix. MG-1 consists of three DGs while MG-2 includes two DGs with different ratings. In the simulation results, the positive and negative signs of $P_{Tie\text{-}line}$ indicate it flows towards MG-1 and MG-2 respectively.

A. Study Cases

1) Case 1: Performance of the scheme on forming the CMG system is evaluated in this case. The simulation results are shown in Fig 6. Initially, the total load of MG-1 is about 1.3MW. Following a 38% load increase in MG-1 at t = 1s, its frequency drops below 49.6Hz at about t = 1.33s, satisfying the coupling conditions (see (4) and (7)). Once the synchronization condition between the voltages at two sides of the ISS fulfills at about t = 1.57s, it closes to form the CMG. Assuming the supervisory scheme is off, a supporting power of about 365kW flows through the tie-line towards MG-1. As a result, power output of MG-1 decreases to 1.44MW while its desirable value ($P^{DSR}_{MG\text{-}1}$) is about 1.62MW. This concern can be efficiently addressed by including the proposed approach. The supervisory scheme switches to Mode 1 by closing the ISS. Consequently, the power output of MG-1 is successfully raised to $P^{DSR}_{MG\text{-}1}$, reducing $P_{Tie\text{-}line}$ to $P^{DSR}_{Tie\text{-}line}$(190kW). Based on (19), the droop slopes of MG-1 are properly updated in intervals of 100ms using a very low bandwidth communication system, as can be seen from Fig. 6.d. To achieve this, the SMF decreases from 1 to 0.72. Moreover, by increasing $P^{Vcap}_{MG\text{-}1}$ by 38% the CMG operates at a higher frequency of about 49.85Hz instead of 49.7Hz, as already demonstrated in Fig. 5.

Note that the transition from Mode 3 to Mode 1 causes the SMF to experience two different trends within this case. By rising the load of MG-1 at t = 1s, the power output of MG-1 increases to a peak of 1.73MW at t = 1.57s which is about 7% larger than $P^{DSR}_{MG\text{-}1}$. Since from this point on the system should be managed under Mode 1, the SMF slightly rises by closing the ISS to reduce the power output of MG-1 to its desired value which is the main target of this mode. At the same time, MG-2 starts supporting MG-1 by providing $P_{Tie\text{-}line}$, dropping power output of MG-1 below $P^{DSR}_{MG\text{-}1}$ at about t = 1.71s. Afterwards, the SMF keeps falling in order to shift the power output up to $P^{DSR}_{MG\text{-}1}$ again. This goal is reached at about t = 5.3s.

2) Case 2: This case validates efficiency of the scheme in lowering $P_{Tie\text{-}line}$ down to zero for a disturbance-free isolation. The simulation results are shown in Fig 7. Let us consider the same CMG system of Case 1 operating at its steady state. Following a 18% load decrease in MG-1 at t = 1s, $P_{Tie\text{-}line}$ drops below the threshold of (10) at t = 1.76s which means the overloading condition of MG-1 is removed and the interconnection is no longer required. Assuming the supervisory scheme is active, its operating mode transits from Mode 1 to Mode 2 to modify the droop coefficients of MG-1 utilizing the SMF of (33), as can be seen from Fig. 7.d. Finally, the controller sends a command to the ISS to open at t = 4.16s when the tie-line power is almost zero. Once the MGs are isolated, the supervisory scheme switches to Mode 3 based on which the droop coefficients are reset to their default values by (35). Also, Fig. 7 shows the outcomes when the scheme is off. Since L2C of MG-1 is still larger than that of MG-2, a supporting power of about 230kW flows towards MG-1 even after violation of (10). Hence, the ISS should open while $P_{Tie\text{-}line}$ is not zero, causing destructive voltage transients due to the derivative term of (14). Note that opening of the ISS is intentionally postponed to t=4.16s to provide a better comparison between on and off states of the scheme.

The transition from Mode 1 to Mode 2 is fulfilled following the load decrease in MG-1. As a result of this reduction, the DGs of MG-1 tend to reduce their output powers as well. Then, the supervisory controller under Mode 1 starts reducing the SMF at t = 1s in order to maintain the power output of MG-1 at $P^{DSR}_{MG\text{-}1}$. This condition carries on till the violation of (10) and the subsequent transition to Mode 2 at t = 1.76s, which dictates the new target of reducing $P_{Tie\text{-}line}$ to zero. Since at this moment MG-1 still receives support from MG-2, the controller commands the DGs of MG-1 to increase their power output through decreasing the SMF. After a few slight variations of the SMF, the ISS can be opened with almost no disturbance at t = 4.16s when the controller is switched to Mode 3. The droop regulato-

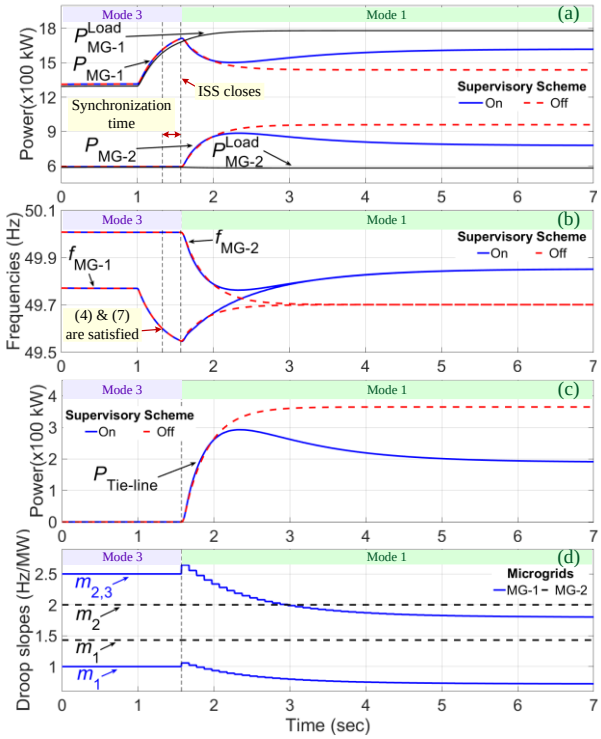

Fig. 6. Simulation results of Case 1.

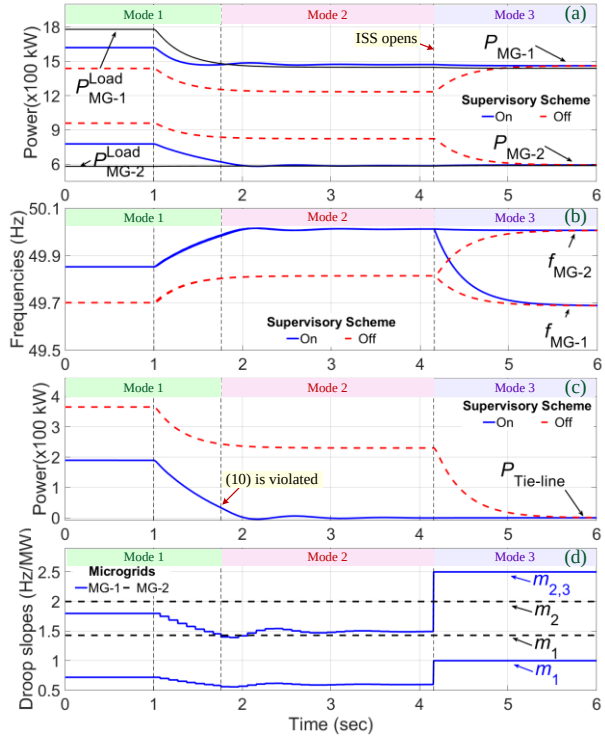

Fig. 7. Simulation results of Case 2.

rs are given back the default values by resetting the SMF to one. As a result, the droop slopes of the DGs in MG-1 are increased, reducing the frequency to about 49.7Hz.

3) Case 3: Operation of the scheme when an overloading occurs in MG-2 is studied in this case. Although the formulation of the scheme is fulfilled assuming a power deficiency in MG-1, similar action can be conducted when the shortfall takes place in MG-2. The simulation results are shown in Fig 8. Following a 62% load increase in MG-2, the coupling conditions are satisfied at about t = 1.53s and the ISS closes at t = 2.07s. Assuming the scheme is off, a supporting power of about 360kW flows towards MG-2 which is about four times larger than $P^{DSR}_{Tie\text{-}line}$ i.e. 100kW. As can be seen from Fig 8, the supervisory scheme can keep power output of MG-2 at $P^{DSR}_{MG\text{-}2}$=1.08MW through properly modifying the droop slopes of MG-2, decreasing the tie-line power to $P^{DSR}_{Tie\text{-}line}$ and raising the frequency to about 49.96Hz.

Similar to Case 1, the SMF experiences two different trends in transiting from Mode 3 to Mode 1. By increasing the load of MG-2 at t = 1s, the power output of MG-2 increases to about 1.17MW at t = 2.07s which is 8.5% larger than $P^{DSR}_{MG\text{-}2}$. At this moment, the operating mode switches to Mode 1 by closing the ISS, raising the SMF slightly to reduce power output of MG-2 to $P^{DSR}_{MG\text{-}2}$. After a very short time, output power of MG-2 decreases considerably due to sharing the total load demand among the DGs of both MGs. Hence, the controller reduces the SMF in order to force the DGs of MG-2 to maintain the power output at $P^{DSR}_{MG\text{-}2}$. The system condition settles at about t=5.6s.

4) Case 4: This case considers the same CMG system of Case 3 operating at its steady state to validate efficiency of the supervisory scheme in implementing a desirable isolation. Following a 30% load decrease in MG-2 at t = 1s, the scheme switches to Mode 2 at about t = 1.16s. Thus, the controller commands the ISS to open at t = 3.78s at which $P_{Tie\text{-}line}$ is successfully decreased to about zero with a SMF of 0.69. The waveforms are shown in Fig 9. It is to be noted that without including the supervisory scheme, a supporting power of about 160kW can flow towards MG-2 even after violation of (10) which may cause destructive transients during the isolation procedure.

Two transition processes, i.e., Mode 1 to Mode 2 and then, Mode 2 to Mode 3, occur in this case. During the first one, the SMF experiences a number of changes in its trend. From t = 1s to t = 1.16s, the SMF decreases to maintain power output of MG-2 at its desired value since the system is operating under Mode 1. From t = 1.16s to t = 1.23s, the reduction of the SMF continues under Mode 2 in order to cancel the tie-line power through increasing power output of MG-2. From this point onwards, the SMF experiences a few variations due to the dynamic response of the system. Eventually, the ISS can open at about t = 3.78s when $P_{Tie\text{-}line}$ settles down at zero. At this moment, the second transition takes place through resetting the droop coefficients to their default values. The frequency of MG-2, consequently, decreases to 49.8Hz since the droop coefficients of the DGs are now increased.

5) Case 5: Figure 10 illustrates the simulation results of the same system of Case 2 when MG-1 experiences a larger load reduction of about 67% at t = 1s. Due to the fact that L2C of MG-1 after the load change is smaller than that of MG-2, $P_{Tie\text{-}line}$ changes its direction towards MG-2, as can be seen from Fig. 10.c. The waveforms prove the capability of the scheme in reducing the tie-line power to zero by transiting to Mode 2 and then, fulfilling a successful isolation at t = 3.97s.

The transition from Mode 1 to Mode 2 takes place in a very short time after the load change at t = 1s. The reduction in the

SMF, already started under Mode 1 to maintain the power

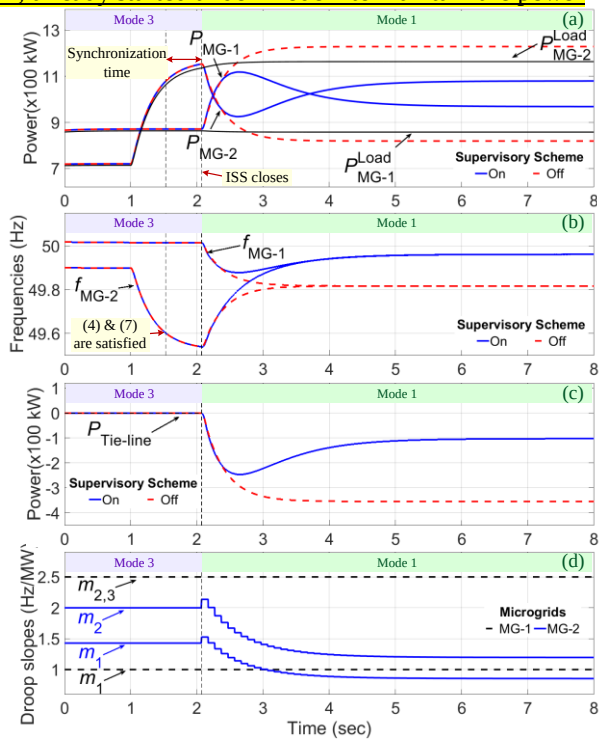

Fig. 8. Simulation results of Case 3.

output of MG-1 at the desired value, carries on till t = 1.28s under Mode 2 to decrease the tie-line power to zero. Due to the severity of the load change, the power output of the MGs experiences variations, causing some trend change in the SMF. The main reasons for this type of oscillations can be found in Section VI.B. Finally, the SMF settles down at a comparatively larger value than it had under Mode 1 with the aim of decreasing the power output of MG-1. Otherwise, a non-zero supporting power can flow towards MG-2, resulting in undesirable disturbances during the isolation. Note that the power curves in Fig. 10a are overlapped since both MGs have similar load demands after the load change at t = 1s. By opening the ISS at t = 3.78s, the operation transits to Mode 3, resetting the droop coefficients to their defaults. The frequency of MG-1 rises to about 50.17Hz as a result of the reduction in the associated droop coefficients.

The simulation outcomes illustrate efficacy of the proposed scheme in coping with active power shortfalls in remote MGs. As already stated in Section II, a few assumptions on large reactive loads are taken into account in order to focus on the main target and to make the paper easy to follow. The issues of accurate sharing of both active and reactive powers will be considered in further research. Note that higher bandwidth bidirectional communication systems are required to properly address this issue.

B. Eigenvalue studies

Small signal analysis of the simulated CMG is presented in this section in order to examine impact of the supervisory coefficient on the stability of the system. Eigenvalues of state matrix of the CMG ($A_{CMG} \in R^{70\times70}$) are derived by taking into account the variation of SMF. Let us consider the CMG with technical parameters shown in Table I. Fig. 11 illustrates traces of the dominant eigenvalues of the CMG when the SMF changes from 1.6 to 0.5 which is the practical range for the

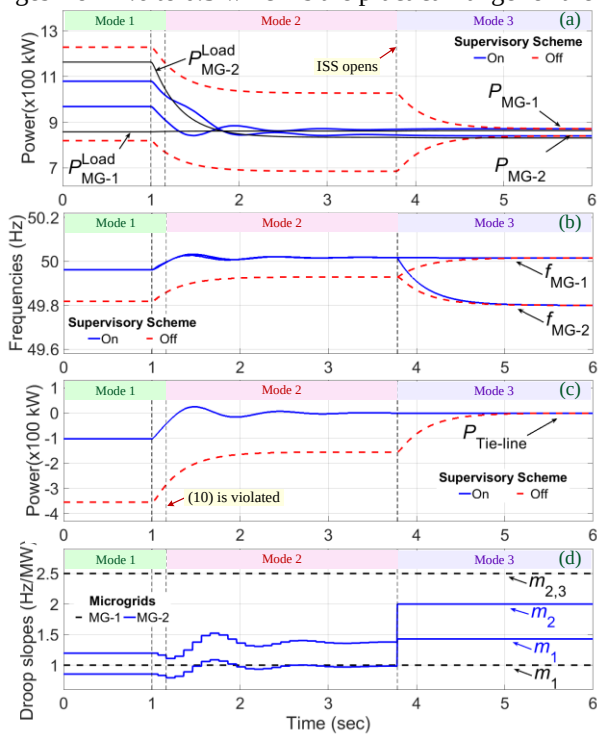

Fig. 9. Simulation results of Case 4.

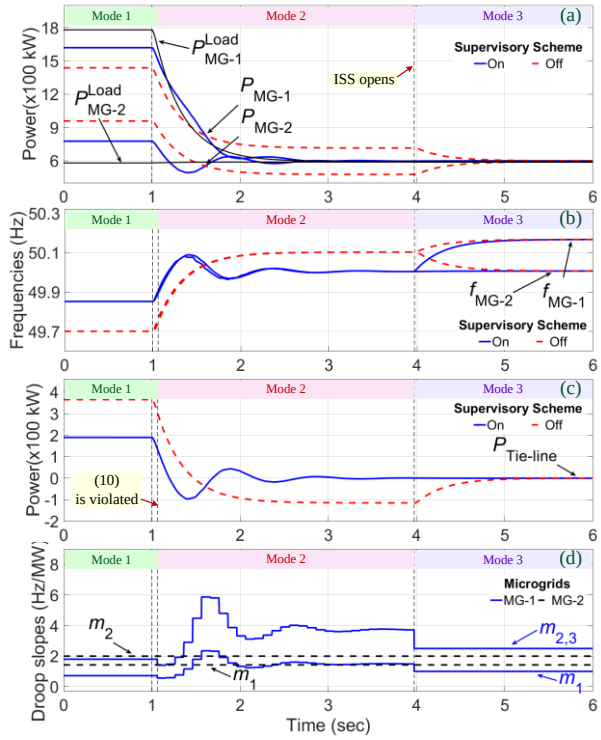

Fig. 10. Simulation results of Case 5.

considered CMG. In most cases, the SMF should be decreased to a value below one to perform the scheme under both Mode 1 and Mode 2, as already shown by the dynamic simulations. It is obvious from Fig. 11 that decreasing the SMF increases the stability of the system as the modes move to the left in the s-plane. However, it is possible for the SMF to rise to a value larger than one, especially during isolation procedure of some

extreme cases such as Case 5 of the previous section. In such

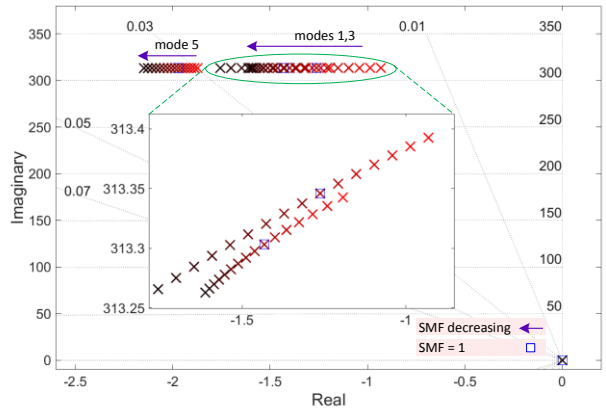

Fig. 11. Trace of dominant modes of the CMG when the SMF decreases from 1.6 to 0.5.

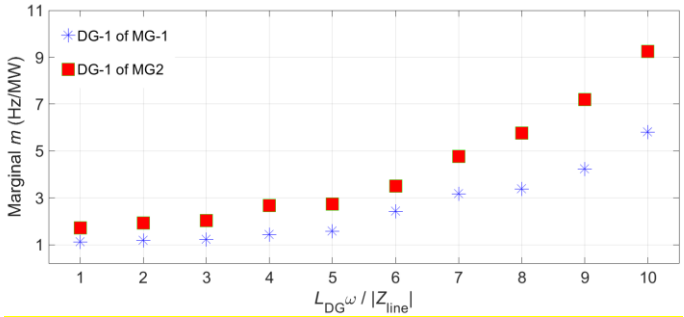

Fig. 12. Marginal droop coefficients of the sample DGs when the ratio of the coupling reactance of the DGs over line impedances varies from 1 to 10.

circumstances, although the eigenvalues move towards the right, the system stability can be maintained as the dominant eigenvalues are still on the left half s-plane. These outcomes fit well with the dynamic response of the system already shown in subsection VI.A.

Along with the discussion in Section II, the impact of selecting adequately high coupling inductances of the DGs on the droop gain stability margins is evaluated for the CMG under study. These marginal values indicate the maximum active power droop coefficients of the DGs, before the CMG faces instability. Fig. 12 demonstrates the marginal droop coefficients of the sample DGs when the ratio $L_{DG}\omega:|Z_{line}|$ varies from 1 to 10. The plots indicate that the sensitivity of the system to different characteristics of the line impedances decreases by increasing the ratio, enhancing droop gain stability margins of the overall system.

The permitted range of variation for the SMF depends mainly on its impacts on the stability of the CMG. This issue is highly influenced by the operating point of each CMG. Limiting the SMF values from the lower side is not of major concern since decreasing this value have positive impacts on the stability of the system, as can be seen from Fig. 11. Note that the SMF should be decreased in most of the cases to achieve the desirable operation of the system. However, the upper boundaries of the SMF should be mainly taken into account due to the fact that increasing the SMF can deteriorate the performance of the system from the stability point of view. Fig. 12 shows the upper limits of the droop coefficients of the DGs for different impedance characteristics of the system calculated by taking advantage of the developed small signal model. Similar pattern can be applied to find the upper limits

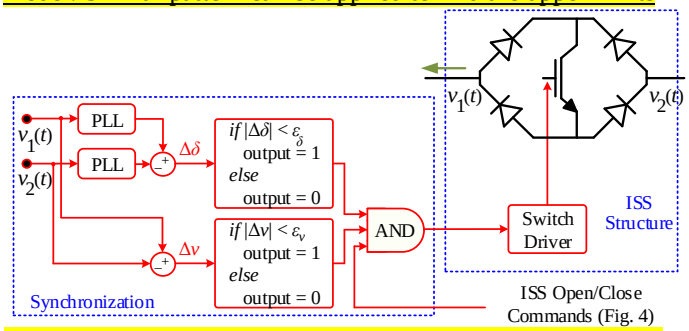

Fig. A1. Per-phase structure of the ISS along with its controlling mechanism.

TABLE I. TECHNICAL PARAMETERS OF THE MGS AND THE CMG.

General parameters: α =0.1, V_{max} = 6.35 kV, V_{min} = 6 kV, f_{max} = 50.5 Hz, f_{min} = 49.5 Hz					
MGs and CMG line parameters: Z_{line} = 0.1 + j 0.1 Ω , $Z_{tie\text{-}line}$ = 0.2 + j 0.2 Ω					
Droop slopes of the MGs					
P^{cap}	MG-1 (P^{cap} = 1.8MW)			MG-2 (P^{cap} = 1.2MW)	
DGs	DG-1	DG-2	DG-3	DG-1	DG-2
m [Hz/MW]	1	2.5	2.5	1.4	2
n [kV/MVAr]	0.3	0.75	0.75	0.42	0.6
L_{DG} [mH]	5	12.5	12.5	7	10

of the SMF considering different operating points of the CMG. For example, this value is about 4.9 for the system studied in Fig. 11.

VII. CONCLUSION

A supervisory control scheme is presented to address the challenges with the ISS-based coupling of remote droop-regulated MGs. The strategy is developed to be applied under three modes, namely Mode 1 that is initiated by forming the CMG to keep the power output of the overloaded MG close to its maximum; Mode 2 that aims to fulfill a successful isolation when the interconnection is not required anymore; and Mode 3 that is activated by opening the ISS to reset default values of the DGs controllers. Several simulation studies are carried out to evaluate performance of the proposed scheme under various conditions. The simulation results illustrate that once the CMG is formed the scheme can desirably control the power output of the MGs by switching to Mode 1. Moreover, success of the scheme in reducing the tie-line power to zero before opening the ISS is shown under various L2C conditions. The obtained results prove that the scheme can effectively achieve the defined goals using a very low bandwidth communication system.

APPENDIX

A. *Data of Simulation Case Studies*

Table I lists the technical parameters of the MGs, considered in the simulation studies.

B. *The ISS Structure*

The ISS is a bidirectional switch through which facilitates power flow towards an overloaded MG. The per-phase schematic of the adopted structure is shown in Fig. A1. This bidirectional device is formed by embedding an IGBT in a

diode bridge. Once the IGBT is turned on, i.e. the ISS closes, the supporting power can flow in either directions in accordance with the droop coefficients of the DGs of the MGs. As already mentioned, the ISS should close when the voltages at its two sides, v_1 and v_2, are synchronized and both (4) and (7) are satisfied (see Fig. 4). This mechanism is also illustrated in Fig. A1 in which $|\Delta\delta|$ and $|\Delta v|$ denote phase and magnitude differences of the voltages respectively and ε is a value sufficiently small to ensure the transient-free interconnection procedure of the MGs. After closing, the ISS maintains this status as long as the coupling is required. Once the controller decides that the interconnection is not required any more, it sends an OFF command to the ISS to open and wait for the next coupling action. Further explanations on the synchronization procedure can be found in [12].

REFERENCES

[1] J. Sachs, O. Sawodny, "A two-stage model predictive control strategy for economic diesel-pv-battery island microgrid operation in rural areas," *IEEE Trans. Sustainable Energy*, vol. 7, no. 3, pp. 903-913, July 2016.

[2] M.M.A. Abdelaziz, H.E. Farag,, E.F. El-Saadany, "Optimum reconfiguration of droop-controlled islanded microgrids," *IEEE Trans. Power Systems*, vol. 31, no. 3, pp. 2144-2153, May 2016.

[3] J. He, Y.W. Li, J.M. Guerrero, F. Blaabjerg, "An islanding microgrid power sharing approach using enhanced virtual impedance control scheme," *IEEE Trans. Power Electronics*, vol. 28, no. 11, Nov. 2013.

[4] P. C. Loh, D. Li, Y. K. Chai, and F. Blaabjerg, "Autonomous operation of hybrid microgrid with AC and DC subgrids," *IEEE Trans. Power Electron.*, vol. 28, no. 5, pp. 2214–2223, May 2013.

[5] H. Gao, Y. Chen, Y. Xu, C. Liu, "Dynamic load shedding for an islanded microgrid with limited generation resources," *IET Gener. Transm. Distrib.*, vol. 10, no. 12, pp. 2953-2961, 2016.

[6] A. Solanki, A. Nasiri, V. Bhavaraju, Y.L. Familiant, Q. Fu, "A new framework for microgrid management: virtual droop control," *IEEE Trans. Smart Grid*, vol. 7, no. 2, pp. 554-566, March 2016.

[7] J. Xiao, L. Bai, , F. Li, H. Liang, C. Wang, "Sizing of energy storage and diesel generators in an isolated microgrid using DFT," *IEEE Trans. Sustainable Energy*, Vol. 5, no. 3, pp. 907-916, July 2014.

[8] S.A. Arefifar, Y.A.R.I. Mohamed, T.H.M. EL-Fouly, "Optimum microgrid design for enhancing reliability and supply-security," *IEEE Trans. Smart Grid*, vol. 4, no. 3, pp. 1567-1575, Sep 2013.

[9] X. Tang, X. Hu, N. Li, W. Deng and G. Zhang, "A novel frequency and voltage control method for islanded microgrid based on multienergy storages," *IEEE Trans. Smart Grid*, vol. 7, no. 1, pp. 410-419, Jan 2016.

[10] Y. Xu, W. Zhang, G. Hug, "Cooperative control of distributed energy storage systems in a microgrid," *IEEE Trans. Smart Grid*, vol. 6, no. 1, pp. 238-248, Jan 2015.

[11] R.H. Lasseter, "Smart distribution: coupled microgrids," *Proceedings of the IEEE*, vol. 99, no. 6, pp. 1074-1082, June 2011.

[12] E. Pashajavid, F. Shahnia, A. Ghosh, "development of a self-healing strategy to enhance the overloading resilience of islanded microgrids," *IEEE Trans. Smart Grid*, DOI 10.1109/TSG.2015.2477601.

[13] E. Pashajavid, A. Ghosh, "A fully decentralized approach for mitigating destructive disturbances in isolating process of remote coupled microgrids," Australasian Universities Power Engineering Conference (AUPEC), Brisbane, Australia, Sep. 2016.

[14] H. Dagdougui, *et al*. "Optimal control of a network of power microgrids using the Pontryagin's minimum principle," *IEEE Trans. Control Systems Technology*, vol. 22, no. 5, pp. 1942–1948, Sep. 2014.

[15] Z. Wang, B. Chen, J. Wang and C. Chen, "Networked microgrids for self-healing power systems," *IEEE Trans. Smart Grid*, vol. 7, no. 1, pp. 310-319, Jan. 2016.

[16] R. Majumder, B. Chaudhuri, A. Ghosh, R. Majumder, G. Ledwich, F. Zare, "Improvement of stability and load sharing in an autonomous microgrid using supplementary droop control loop," *IEEE Trans. Power Systems*, vol. 25, no. 2, pp. 796-808, May 2010.

[17] Q. Sun, J. Zhou, J.M. Guerrero, H. Zhang, "Hybrid three-phase/single-phase microgrid architecture with power management," *IEEE Trans. Power Electronics*, vol. 30, no. 10, pp. 5964-5977, Oct 2015.

[18] R. Majumder, A. Ghosh, G. Ledwich, F. Zare, "Power management and power flow control with back-to-back converters in a utility connected microgrid," *IEEE Trans. Power Systems*, vol. 25, no. 2, pp. 821-834, May 2010.

[19] M.J. Hossain, M.A. Mahmud, F. Milano, S. Bacha, A. Hably, "Design of robust distributed control for interconnected microgrids," *IEEE Trans. Smart Grid*, DOI 10.1109/TSG.2015.2502618, 2015.

[20] T. Friedli, J. W. Kolar, J. Rodriguez and P. W. Wheeler, "Comparative evaluation of three-phase ac–ac matrix converter and voltage dc-link back-to-back converter systems," *IEEE Transactions Industrial Electronics*, vol. 59, no. 12, pp. 4487-4510, Dec 2012.

[21] Y. Han, H. Li, P. Shen, E.A.A. Coelho, J.M. Guerrero, "Review of active and reactive power sharing strategies in hierarchical controlled microgrids," *IEEE Transactions Power Electronics*, vol. 32, no. 3, pp. 2427-2451, March 2017.

[22] I. P. Nikolakakos, H.H. Zeineldin, M.S. El-Moursi, N.D. Hatziargyriou, "Stability Evaluation of Interconnected Multi-Inverter Microgrids Through Critical Clusters," *IEEE Trans. Power Systems*, vol. 31, no. 4, pp. 3060-3072, July 2016.

[23] E. Pashajavid, F. Shahnia, A. Ghosh, "Interconnection of two neighboring autonomous microgrids based on small signal analysis," 9th IEEE Int. Conf. on Power Electronics Asia (ICPE-ECCE), Korea, 2015.